

PNIPAAm-Modified Nanoporous Colloidal Films with Positive and Negative Temperature Gating

Olga Schepelina and Ilya Zharov*

Department of Chemistry, University of Utah, Salt Lake City, Utah 84112

Received July 5, 2007. In Final Form: September 14, 2007

The surface of nanopores in colloidal films, assembled from 205 nm silica spheres, was modified with poly(*N*-isopropylacrylamide), PNIPAAm, brushes using surface-initiated ATRP. The polymer thickness inside nanopores was controlled by the polymerization time. The diffusion through PNIPAAm-modified colloidal films was measured using cyclic voltammetry and studied as a function of temperature and polymer brush thickness. Nanopores modified with a thin PNIPAAm brush exhibited a positive gating behavior, where diffusion rates increased with increasing temperature. Nanopores modified with a thick PNIPAAm layer showed a negative gating behavior where diffusion rates decreased with increasing temperature. The observed temperature response is consistent with two transport mechanisms, one in which molecules diffuse through the nanopores whose volume increases with increasing temperature as the PNIPAAm brush collapses onto the nanopore surface (positive gating) and the second one where molecules diffuse through the porous PNIPAAm that fills the entire nanopore opening and collapses onto itself, becoming hydrophobic and impermeable (negative gating).

Introduction

We wish to report the preparation and temperature-responsive behavior of nanoporous colloidal films modified with poly(*N*-isopropylacrylamide), PNIPAAm, brush prepared by surface-initiated atom transfer radical polymerization (ATRP). Our general strategy is based on the use of silica colloidal crystals¹ as a nanoporous matrix that forms via self-assembly, contains ordered arrays of three-dimensional interconnected nanopores, and can be surface-modified to produce responsive porous materials.

Recently, we showed that chemical selectivity can be introduced into nanoporous colloidal films by surface modification with chargeable groups such as amines^{2,3} or sulfonic acids⁴ and with neutral chiral selector moieties.^{5,6} Another approach to controlling the transport through colloidal nanopores is by modifying their surfaces with responsive polymers. Because temperature-responsive polymers provide a straightforward way of studying polymer-gated nanopores, we decided to modify the surface of colloidal nanopores with PNIPAAm, a well-known thermo-responsive polymer.⁷

PNIPAAm has been used to modify porous polycarbonate⁸ and polyethylene⁹ to prepare temperature-responsive membranes.¹⁰ The most common approach used to date for the preparation of temperature-responsive porous membranes was grafting of premade responsive polymers onto plasma-activated

membrane surface^{8,11} as well as UV light-initiated pore-filling radical polymerization¹² in porous glass¹³ and silica.¹⁴ In a recent study,¹⁵ a new approach to formation of thermally responsive silica/PNIPAAm hybrid mesoporous materials was described. In this method, PNIPAAm was incorporated into polymerizing silica network using a coupling agent.

It has been demonstrated that transport selectivity could be built into micrometer- and submicrometer-sized pores using grafted macromolecules that respond to other environmental stimuli,¹⁶ including pH,^{17,18} light,¹⁹ and ions.²⁰ Gold-plated nanotubes have been modified with biopolymers to provide chiral selectivity to the transport through such nanotubes.²¹

Recently, we demonstrated²² that surface-initiated^{23–27} atom transfer radical polymerization (ATRP)^{28,29} allows preparation of poly(acryl amide)-modified nanopores inside colloidal films in a uniform and reproducible fashion without perturbing the colloidal crystal lattice. In the present work we describe surface-initiated ATRP of *N*-isopropylacrylamide^{30,31} inside highly

* To whom correspondence should be addressed. E-mail: i.zharov@utah.edu.

- (1) Wong, S.; Kitaev, V.; Ozin, G. A. *J. Am. Chem. Soc.* **2003**, *125*, 15589–15598.
- (2) Newton, M. R.; Bohaty, A. K.; White, H. S.; Zharov, I. *J. Am. Chem. Soc.* **2005**, *127*, 7268–7269.
- (3) Newton, M. R.; Bohaty, A. K.; Zhang, Y.; White, H. S.; Zharov, I. *Langmuir* **2006**, *22*, 4429–4432.
- (4) Zharov, I. Smith, J. J. Submitted for publication.
- (5) Cichelli, J.; Zharov, I. *J. Am. Chem. Soc.* **2006**, *128*, 8130–8131.
- (6) Cichelli, J.; Zharov, I. *J. Mater. Chem.* **2007**, *17*, 1870–1876.
- (7) *Stimuli-Responsive Water Soluble and Amphiphilic Polymers*; McCormick, C. L., Ed.; Oxford University Press: New York, 2001.
- (8) Xie, R.; Chu, L.-Y.; Chen, W.-M.; Xiao, W.; Wang, H.-D.; Qu, J.-B. *J. Membr. Sci.* **2005**, *258*, 157–166.
- (9) Geismann, C.; Yaroshchuk, A.; Ulbricht, M. *Langmuir* **2007**, *32*, 76–83.
- (10) Zhang, L.; Xu, T.; Lin, Z. *J. Membr. Sci.* **2006**, *281*, 491–499.

- (11) Li, Y.; Chu, L.-Y.; Zhu, J. H.; Wang, H.-D.; Xia, H.-L.; Chen, W.-M. *Ind. Eng. Chem. Res.* **2004**, *43*, 2643–2649.
- (12) Peng, T.; Cheng, Y.-L. *J. Appl. Polym. Sci.* **1998**, *70*, 2133–2142.
- (13) Li, S. K.; D'Emanuele, A. *J. Controlled Release* **2001**, *75*, 55–67.
- (14) Rama Rao, G. V.; Lopez, G. *Adv. Mater.* **2000**, *12*, 1692–1695.
- (15) Fu, Q.; Rama, R. G. V.; Ward, T. L.; Lu, Y.; Lopez, G. P. *Langmuir* **2007**, *23*, 170–174.
- (16) Ito, Y.; Park, Y. S. *Polym. Adv. Technol.* **2000**, *11*, 136–144.
- (17) Smuleac, V.; Butterfield, D. A.; Bhattacharyya, D. *Chem. Mater.* **2004**, *16*, 2762–2771.
- (18) Ito, Y.; Park, Y. S.; Imahishi, Y. *Langmuir* **2000**, *16*, 5376–5381.
- (19) Ito, Y.; Park, Y. S.; Imahishi, Y. *Macromolecules* **1998**, *31*, 2606–2610.
- (20) Yamaguchi, T.; Ito, T. *J. Am. Chem. Soc.* **2004**, *126*, 6202–6203.
- (21) Lee, S. B.; Mitchell, D. T.; Trofin, L.; Nevanen, T. K.; Söderlund, H.; Martin, C. R. *Science* **2002**, *296*, 2198–2201.
- (22) Schepelina, O.; Zharov, I. *Langmuir* **2006**, *22*, 10523–10527.
- (23) Edmondson, S.; Osborne, V. L.; Huck, W. T. S. *Chem. Soc. Rev.* **2004**, *33*, 14–22.
- (24) *Polymer Brushes: Synthesis, Characterization, Applications*; Advincula, R. A., Ed.; Wiley-VCH Verlag: New York, 2004.
- (25) Ejaz, M.; Tsujii, Y.; Fukuda, T. *Polymer* **2001**, *42*, 6811–6815.
- (26) Huang, X.; Wirth, M. J. *Anal. Chem.* **1997**, *69*, 4577–4580.
- (27) Xia, D.; Wirth, M. J. *Macromolecules* **2002**, *35*, 2919–2925.
- (28) Wang, J.; Matyjaszewski, K. *Macromolecules* **1995**, *28*, 7901–7910.
- (29) Pyun, J.; Kowalewski, T.; Matyjaszewski, K. *Macromol. Rapid Commun.* **2003**, *24*, 1043–1059.
- (30) Kizhakkedathu, J. K.; Norris-Jones, R.; Brooks, D. E. *Macromolecules* **2004**, *37*, 734–743.

ordered nanopores in colloidal films assembled from 205 nm silica spheres. Using cyclic voltammetry to measure diffusion through the resulting polymer-modified nanopores we demonstrate the ability to easily control the polymer brush thickness by varying polymerization time and describe the temperature response of the resulting composite nanoporous films as a function of the PNIPAAM brush thickness.

Experimental Section

Materials and Reagents. Copper(I) chloride (anhydrous, 99.99%), *N,N,N',N',N''*-pentamethyldiethylenetriamine (PMDETA, 99%), and tetraethyl orthosilicate (TEOS, 99.99%) were obtained from Aldrich and used as received. *N*-Isopropylacrylamide (NIPAAM, 99%) was obtained from Polysciences, Inc. and used as received. 1-(Trichlorosilyl)-2-[*m/p*-(chloromethyl) phenyl] ethane was obtained from Gelest as a mixture of isomers. Hexaamineruthenium(III) chloride, $[\text{Ru}(\text{NH}_3)_6]\text{Cl}_3$ (99%, Strem Chemicals), 1,1'-ferrocenedimethanol, $\text{Fc}(\text{CH}_2\text{OH})_2$ (98%, Aldrich), and potassium chloride (99%, Mallinckrodt) were used as received. Acetonitrile (Mallinckrodt) was distilled before using. Water (18 $\text{M}\Omega\cdot\text{cm}$) was obtained from a Barnsted "E-pure" water purification system.

Preparation and Modification of Silica Spheres in Solution. Silica nanoparticles were prepared by the method of Stober et al.³² A total of 22 mL of TEOS was added to 228 mL of absolute ethanol. The solution was rapidly poured into a stirred mixture of 13 mL of ammonia and 144 mL of water in 93 mL of absolute ethanol at room temperature. The final concentrations of the reagents were 0.2 M TEOS, 0.4 M ammonia, and 17 M water. After the reaction mixture was stirred for 18 h, the spheres were isolated by repeated centrifugation and resuspension in absolute ethanol. The diameter of the spheres was found to be 205 ± 5 nm using scanning electron microscopy (SEM).

Functionalization of silica spheres suspended in acetonitrile was achieved by treatment with 1.5-fold excess of 1-(trichlorosilyl)-2-[*m/p*-(chloromethyl)phenyl]ethane for 18 h at 70 °C. The particles were isolated via centrifugation and washed by 4 cycles of centrifugation and resuspension in acetonitrile, MeOH, CH_2Cl_2 , and acetone in order to remove any adsorbed initiator. To determine the surface coverage of the initiator-modified silica spheres known concentration solutions of 1-(trichlorosilyl)-2-[*m/p*-(chloromethyl)phenyl]ethane were prepared, and the extinction coefficient was determined to be $\epsilon = 2807 \text{ M}^{-1}$ at 242 nm. Next, UV spectra were obtained for colloidal solutions of silica spheres modified with initiator moieties (0.054 g in 10 mL of CHCl_3 for the initial measurement and subsequently diluted). The surface coverage was calculated based on the absorbance at 242 nm and using a 2.07 g/cm^3 density for silica spheres.

Next, silica spheres modified with initiator moieties (1.83 g) were dispersed in a 7:3 mixture of MeOH and water (9 mL). The MeOH/water mixture was degassed by passing a continuous stream of N_2 through the stirred solution (1 h). The polymerization solution was prepared as follows: the organometallic catalyst was formed in nitrogen atmosphere by adding CuCl (26.2 mg, 0.265 mmol) and PMDETA (0.28 mL, 1.3 mmol) to 10 mL of a 7:3 mixture of MeOH and water. The mixture was sonicated for 3–4 min to facilitate formation of the CuCl/PMDETA complex. Next, 3 g (0.0265 mol) of the monomer was added to the mixture and degassed with a stream of dry N_2 (40 min). Then, the mixture was added to the silica suspension. The mixture was then stirred at room temperature. Periodically, samples were taken using a syringe. The polymer-modified silica spheres were washed with methanol and water by repeated suspension and centrifugation.

Pt Microdisk Electrodes. Pt microdisk electrodes (25 μm in diameter) shrouded in glass were prepared by first attaching a 1.0 mm diameter Cu wire (Alfa Aesar) to a 25 μm diameter Pt wire using Ag paint (DuPont). The Pt wire was then flame sealed in a

glass capillary, the capillary was bent into a U shape, and the middle was cut orthogonal to the length of the capillary with a diamond saw to expose the Pt disk. The resulting electrodes were polished with Microcut Paper disks (Buehler), from 240 to 1200 grit in succession, until the surface was free from visible defects.

Preparation of Initiator-Modified Colloidal Films. Colloidal films were deposited on the electrode surfaces and glass slides by placing the electrodes and glass slides vertically in a 1.5 wt % colloidal solution of 205 nm silica spheres in ethanol and letting the solvent evaporate for 2–3 days in a vibration-free environment. The 1.5 wt % silica spheres solution produced 35-layer films with a thickness of ca. 7 μm as determined by SEM.

The surface of the silica spheres assembled into colloidal films on the Pt electrodes was modified by immersing the electrodes under nitrogen in dry acetonitrile containing 0.06 M of 1-(trichlorosilyl)-2-[*m/p*-(chloromethyl)phenyl]ethane. The reaction proceeded at 70 °C for 18 h. After modification, the electrodes were soaked and rinsed with dry acetonitrile.

Surface-Initiated ATRP of NIPAAM in Colloidal Films. To grow PNIPAAM brush inside colloidal films, a NIPAAM polymerization solution was prepared (as described above). The electrodes with initiator-modified colloidal films were immersed into the polymerization mixture by hanging down vertically into the flask under N_2 atmosphere. The reaction mixture was stirred at room temperature. The polymerization time was varied from 15 to 90 min. After reaction, the electrodes were rinsed with MeOH and water.

Cleavage of PNIPAAM from Silica Surface. The colloidal films deposited on glass slides were modified with initiator moieties followed by surface-initiated polymerization using the NIPAAM polymerization solution as described above. After polymerization the glass slides were placed in water for 1 h. To isolate the polymer the modified colloidal films were removed from the glass slides and treated with HF following a previously reported procedure.^{33,34}

Characterization. The molecular flux across the colloidal film was measured voltammetrically using a Par model 175 Universal Programmer and Dagan Cornerstone Chem-Clamp potentiostat. The voltammetric response of the bare and colloidal- and polymer-modified colloidal electrodes was measured in aqueous solutions of either 5.1 mM $\text{Ru}(\text{NH}_3)_6^{3+}$ or 1.6 mM $\text{Fc}(\text{CH}_2\text{OH})_2$ and 0.2 M KCl as supporting electrolyte. Aqueous solutions were prepared using 18 $\text{M}\Omega\cdot\text{cm}$ water and purged with nitrogen to remove dissolved oxygen. Dynamic light scattering (Brookhaven ZetaPALS, measurements conducted in water at 25 °C) and scanning electron microscopy (Hitachi S3000-N, measurements conducted after gold coating of the samples) were employed to perform size characterization of polymer-modified silica spheres. UV spectra were recorded using an Ocean Optics USB2000 instrument. The AFM experiments were performed using a BioScope II Atomic Force Microscope (Veeco). A Bruker Reflex-III MALDI-TOF instrument was used to obtain mass spectra of the cleaved polymer.

Temperature Response Measurements. To perform electrochemical measurements at varied temperatures an immersion circulator with a temperature controller (VWR) was used. The circulator was connected to an external jacketed beaker. To measure temperature response for PNIPAAM-modified nanoporous colloidal films, a solution of the redox species was placed into the beaker and maintained at a constant temperature during the electrochemical measurements.

Results and Discussion

Surface-Initiated Polymerization on Silica Spheres in Solution. An important advantage of using self-assembled colloidal films as nanoporous membranes is in the ability to study the surface modification of the silica spheres in colloidal solution with the assumption that similar processes take place on silica sphere surfaces after their assembly into the colloidal

(31) Jones, D. M.; Smith, J. R.; Huck, W. T. S.; Alexander, C. *Adv. Mater.* **2002**, *14*, 1130–1134.

(32) Stober, W.; Fink, A.; Bohn, E. J. *Colloid Interface Sci.* **1968**, *26*, 62–69.

(33) Nystrom, D.; Antoni, P.; Johansson, M.; Whittaker, M.; Hult, A. *Macromol. Rapid Commun.* **2005**, *26*, 524–528.

(34) Werne, T.; Patten, T. E.; *J. Am. Chem. Soc.* **2001**, *123*, 7497–7505.

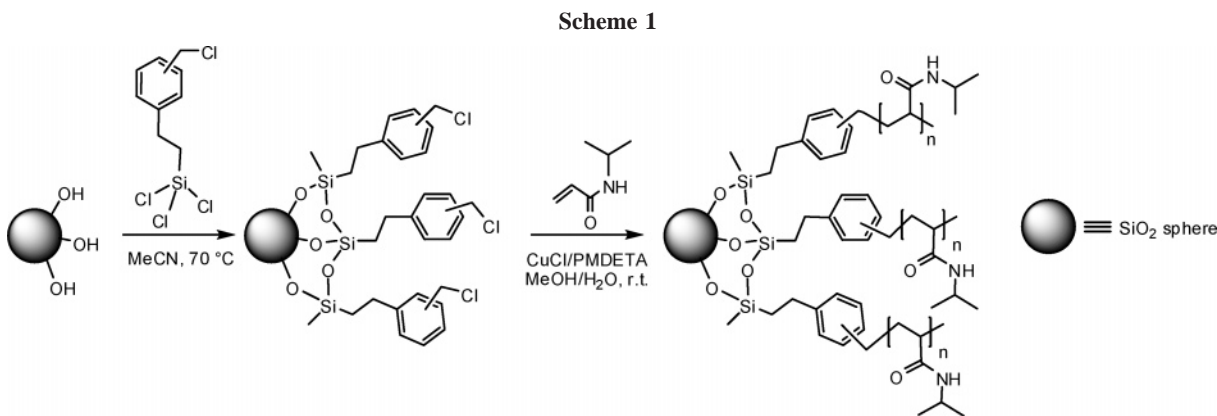


Table 1. Silica Sphere Diameter (d) and Polymer Brush Thickness (Δr) as a Function of Polymerization Time

polymerization time, min	DLS		SEM	
	d , nm	Δr , nm	d , nm	Δr , nm
0	207 \pm 2	0	205 \pm 5	0
15	230 \pm 4	12	210 \pm 6	3
25	250 \pm 10	22	218 \pm 6	7
90	282 \pm 12	38	235 \pm 8	15

crystal. Thus, in order to model the polymerization that would take place inside the colloidal nanopores, we modified 205 nm diameter silica spheres with initiator molecules in solution (Scheme 1). The number of initiator moieties, determined by UV spectroscopy, was ca. 4 molecules/nm², which corresponds to a near monolayer coverage³⁵ of the surface with initiator moieties. The resulting modified silica spheres were treated with *N*-isopropylacrylamide in the presence of copper(I) chloride and PMDETA to form the polymer brushes (Scheme 1). Formation of the polymer was confirmed by IR, which showed signals at 1700 and 3200 cm⁻¹ characteristic of amide groups and at 2900 cm⁻¹ corresponding to the alkyl C–H groups.

To monitor polymer growth on silica spheres in solution as a function of polymerization time we measured the sphere diameters before and after polymerization using dynamic light scattering (DLS) and scanning electron microscopy (SEM) and calculated the polymer brush thickness. The results of these measurements are shown in Table 1. The thickness of the polymer brushes determined by DLS is significantly larger compared to that determined by SEM, which is likely the result of the polymer brush hydration leading to an extended polymer conformation (when measured by DLS in an aqueous solution) in contrast to the collapsed conformation in the dry state (when measured by SEM). Both methods demonstrate the growth of the polymer with time, but the results obtained by DLS are more relevant for the transport measurements described below. For the colloidal films formed from 205 nm silica spheres the distance from the pore center to the nearest silica sphere surface is 16 nm. Thus, it is expected that an almost complete filling of the pores would be achieved after 15 min of polymerization, assuming a similar polymerization rate and uniform surface coverage.

Surface-Initiated Polymerization Inside the Colloidal Film.

In order to determine if the colloidal crystal lattice would remain unperturbed by surface polymerization, we performed ATRP of NIPAAm on 7 μ m thin colloidal films assembled on glass slides using 1.5 wt % solution of 205 nm silica spheres. The surface of the silica spheres was modified with the initiator moieties (Scheme 1), and polymerization of *N*-isopropylacrylamide was

performed for 15 min. The images of the resulting hybrid colloidal/PNIPAAm film are shown in Figure 1. It is clear that the colloidal lattice remained intact, although some silica spheres have been removed from the top layer. It is also apparent from Figure 1 that no thick polymer film is formed over the colloidal crystal and that colloidal nanopores are still present.

Next, we assembled the colloidal films on the surface of eight Pt microelectrodes shrouded in glass, modified their surfaces with initiator moieties, and performed polymerization of *N*-isopropylacrylamide on the electrodes while removing them from solution after different periods of time. We then measured the limiting current of Ru(NH₃)₆³⁺ and Fc(CH₂OH)₂ using these polymer-modified electrodes and compared the current to that before polymerization. The relative limiting current measured for the electrodes after a short polymerization time (15 min) decreased significantly, which suggests that a polymer brush has been formed inside the nanopores. Using the formula described earlier,²² the thickness of the brush after 15 min of polymerization, calculated using the change in limiting current (Table 2), is 9.3 nm, similar to that found for polymerization on silica spheres in solution. In contrast to this result, the limiting current for colloidal film electrodes after a long polymerization time (i.e., 90 min)

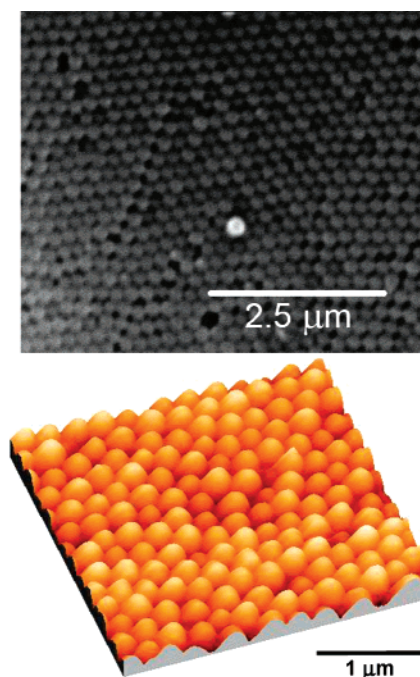


Figure 1. SEM (top) and AFM (bottom) image of the colloidal film assembled from 205 nm silica spheres after surface modification with initiator moieties and ATRP polymerization of *N*-isopropylacrylamide for 15 min.

(35) Jal, P. K.; Patel, S.; Mishra, B. K. *Talanta* **2004**, *62*, 1005–1028, and references therein.

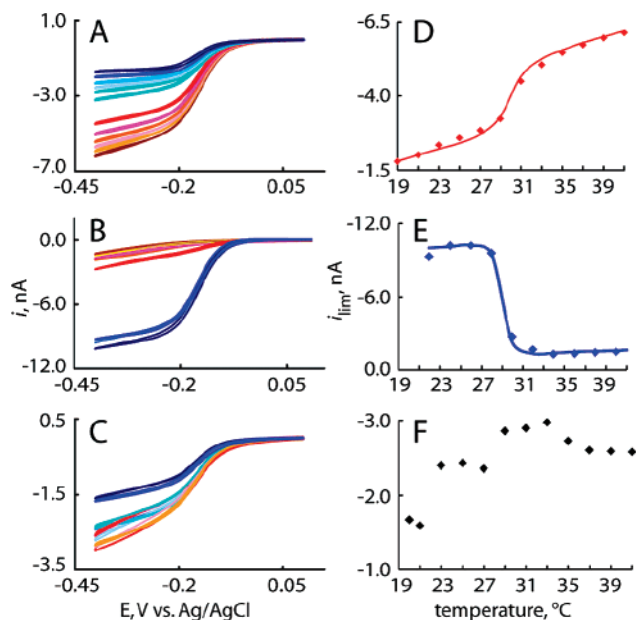


Figure 2. Representative voltammograms ($\text{Ru}(\text{NH}_3)_6^{3+}$) of colloidal film Pt electrodes after polymerization for (A) 15, (B) 90, and (C) 20 min at different temperatures. Voltammograms corresponding to temperatures below 30 °C are shown in blue, and those for temperatures above 30 °C are shown in yellow and red. Limiting current of ($\text{Ru}(\text{NH}_3)_6^{3+}$) as a function of increasing temperature for PNIPAAm–colloidal film Pt electrodes after polymerization for (D) 15, (E) 90, and (F) 20 min.

Table 2. Relative Limiting Current of Colloidal Film Pt Electrodes as a Function of Polymerization Time, and Geometrical Characteristics of Resulting Polymer-Modified Colloidal Nanopores

polymerization time, min	$i_{\text{lim}}/i_{\text{lim}}(0)$	ϵ'	Δr , nm
15	0.26	0.068	9.3
25	0.21	0.055	10.0
90	0.73	(0.19)	(3.0)

is much higher than that after 15 min polymerization and similar to that for unmodified colloidal film electrodes. As described above, polymerization for 90 min on silica spheres in solution results in a polymer brush of ca. 38 nm thickness. This suggests that the limiting current calculations, which assume no transport through the polymer brush, cannot be used in this case and that a polymer of a different morphology is formed when polymeric chains become long enough for the polymer brushes growing from nanopore surfaces to interpenetrate each other (see below). Finally, polymerization inside the colloidal films for 25 min leads, based on the limiting current data, to 10 nm thick polymer brushes, which is ca. 2 times smaller compared to that observed for the polymerization in colloidal solution. This may also suggest that a polymer of a different morphology is formed.

Temperature-Responsive Behavior of the PNIPAAm-Modified Colloidal Films. Next, we investigated the temperature response for PNIPAAm-modified nanoporous colloidal films prepared at different polymerization times using cyclic voltammetry of $\text{Fc}(\text{CH}_2\text{OH})_2$ and $\text{Ru}(\text{NH}_3)_6^{3+}$. As can be seen in Figure 2, the limiting current for PNIPAAm-modified colloidal film electrodes is affected by temperature. For all colloidal film electrodes the limiting current slightly increases with increasing temperature as a result of increasing diffusion coefficient.³⁶ Most importantly, we observed two clearly distinguishable types of temperature responses. For nanoporous films modified with a

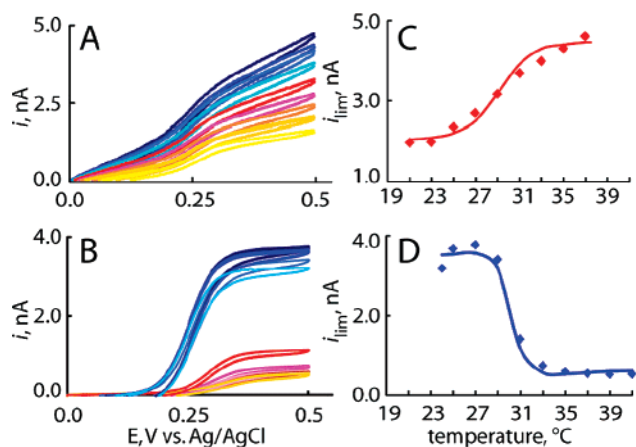


Figure 3. (A and B) Representative voltammograms and (C and D) plots of $\text{Fc}(\text{CH}_2\text{OH})_2$ limiting current as a function of temperature for PNIPAAm–colloidal film Pt electrodes after polymerization for 15 and 90 min, respectively.

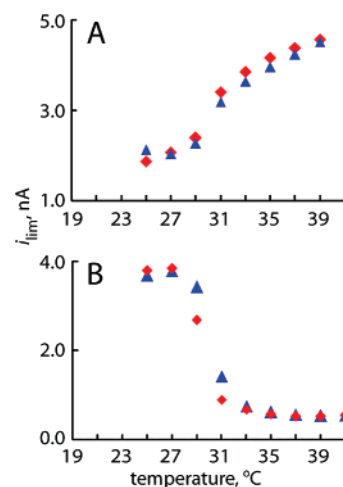


Figure 4. Limiting current as a function of increasing (red) and decreasing (blue) temperature for PNIPAAm–colloidal film Pt electrodes ($\text{Fc}(\text{CH}_2\text{OH})_2$) after polymerization for (A) 15 and (B) 90 min.

thin polymer brush (polymerization for 15 min) the limiting current increased with increasing temperature with a gradual change centered at ca. 29 °C (Figure 2A,D). For colloidal films modified with thick polymer brushes (polymerization for 90 min) a reverse response was observed where the limiting current decreased with increasing temperature with a sharp change at ca. 29 °C (Figure 2B,E). For both types of temperature responses the gating was quite complete, i.e., the diffusion rates changed between almost zero and values similar to those observed for unmodified colloidal films. Polymer brushes with an intermediate thickness, such as those obtained after 20–25 min polymerization, did not show a clear trend in the temperature response (Figure 2C,F).

To verify that the observed changes in the molecular transport do not result from electrostatic effects,^{2,3} we examined the temperature response of PNIPAAm–colloidal film electrodes for a neutral molecule, $\text{Fc}(\text{CH}_2\text{OH})_2$. These experiments (Figure 3) showed temperature-responsive behavior similar to that obtained for positively charged $\text{Ru}(\text{NH}_3)_6^{3+}$.

The temperature-dependent change in the limiting current was reversible for both types of polymer brushes and for both redox species (Figure 4). The nanoporous polymer-modified colloidal films could be cycled between low and high temperatures without apparent loss of responsiveness, as shown in Figure 5. It appears

(36) Cussler, E. L. *Diffusion. Mass Transfer in Fluid Systems*, 2nd ed.; Cambridge University Press: New York, 1997.

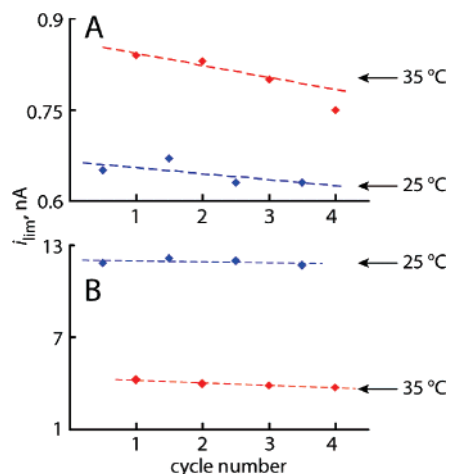


Figure 5. Limiting current at low (blue) and high (red) temperature for PNIPAAm-colloidal film Pt electrodes ($\text{Fc}(\text{CH}_2\text{OH})_2$) after polymerization for (A) 15 and (B) 90 min as a function of temperature cycling.

that while the transport rates through the nanoporous films carrying a thick polymer brush did not change with temperature cycling (Figure 5B), the transport rates through the nanopores modified with a thin polymer brush decreased with temperature cycling (Figure 5A).

To verify that the temperature-responsive behavior described above results from the nanopore surface modification, glass-shrouded Pt microelectrodes not carrying a colloidal film were treated with initiator molecules followed by the NIPAAm polymerization for 90 min. The resulting electrodes did not show a temperature-responsive behavior (except for a small increase in transport rates resulting from the change in the diffusion coefficients). In addition, the glass surface of the Pt electrodes was deactivated by treating with 3-cyano-propyldimethylchlorosilane to make sure that the glass surface has not been modified with the polymer. The colloidal films were deposited onto the surface of the modified electrodes using 1.5 wt % of silica spheres in ethanol. Next, the colloidal film deposited on the electrode was modified with the initiator followed by surface-initiated polymerization on NIPAAm for 90 min. The limiting current for this electrode showed the temperature response similar to that describe above, i.e., the limiting current decreased with increasing temperature.

The molecular weight of the PNIPAAm chains formed inside the colloidal nanopores can be estimated based on the polymer thickness measured by DLS of polymer-modified silica spheres in solution, assuming that the chains are fully extended²⁴ and taking the length of the monomeric unit to be ca. 0.25 nm. For polymer brushes obtained after 15 min of polymerization the MW can be estimated as ca. 5400 Da, while for those obtained after 90 min it is ca. 17 000 Da.

This prediction is in agreement with the observed transition behavior. Although the transition temperature of ca. 29 °C was obtained for both types of colloidal films, the response for the films modified with a short polymer brush (15 min polymerization time) is gradual while for the films modified with a long polymer brush (90 min polymerization time) the response is sharp. This observation indicates that the MW of the surface-attached polymer increased significantly. Indeed, a similar MW-dependent transition behavior was recently reported for surface-grafted PNIPAAm.^{37,38}

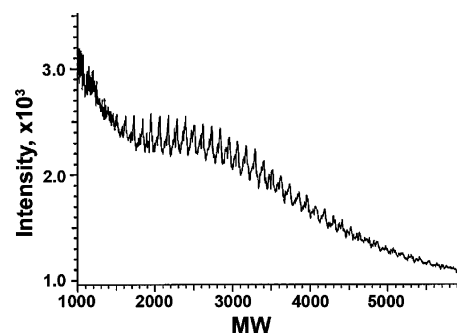


Figure 6. MALDI-TOF MS of PNIPAAm obtained after 15 min polymerization inside the colloidal nanopores and cleaved from the colloidal film surface as described in the text.

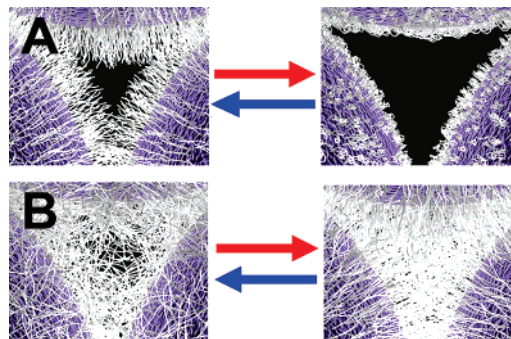


Figure 7. Schematic representation of processes that occur upon heating and cooling of a (A) PNIPAAm brush (15 min polymerization) and (B) PNIPAAm gel (90 min polymerization) inside a colloidal nanopore.

To directly measure the molecular weights of PNIPAAm prepared inside the colloidal nanopores we cleaved the polymers from the silica surface using HF. The amount of the polymers obtained this way was not sufficient for GPC studies. However, we were able to obtain a MALDI-TOF MS spectrum for the short polymer (Figure 6). According to the spectrum these brushes have a molecular weight of around 2700 Da with a rather broad distribution. Both lower than expected MW and broader than expected MW distribution may be the result of NIPAAm decomposition under the MALDI conditions and/or of the nanopore geometry. The polymeric material released from the colloidal films surface after polymerization for 90 min showed low solubility, and we were unable to obtain its MALDI-TOF MS spectra.

The experimental results described above are consistent with two types of PNIPAAm morphology inside colloidal nanopores that lead to two types of molecular transport through these nanopores. When *N*-isopropylacrylamide is polymerized for a short period of time it forms a dense brush (Figure 7A). Transport through such nanopores mainly occurs in the polymer-free volume of the nanopores. The thickness of the polymer brush formed after 15 min polymerization has been calculated to be 12 nm (see above), thus blocking a large portion of the nanopore volume. Increasing the temperature leads to the conformational changes in the polymer chains inside the brush which shrinks to the nanopore walls, providing a larger volume for diffusion (Figure 7A).

In contrast, when polymerization is conducted for a sufficiently long time (over 30 min) polymer chains growing from the opposite nanopore walls become long enough to interpenetrate and possibly cross-link. The latter speculation is based on the low solubility of this polymer released from the silica surface. The resulting structure is highly porous and allows diffusion of water and small molecules at temperatures below LCST (Figure 7B). When

(37) Plunkett, K. N.; Zhu, X.; Moore, J. S.; Leckband, D. E. *Langmuir* **2006**, *22*, 4259–4266.

(38) Yim, H. H.; Kent, M. S.; Mendez, S.; Lopez, G. P.; Satija, S.; Seo, Y. *Macromolecules* **2006**, *39*, 3420–3426.

the temperature is increased above LCST, the densely packed polymer inside the nanopores becomes dehydrated and impermeable to aqueous permeants (Figure 7B). There is an intermediate polymer size and density region showing a mixed temperature response (Figure 2F).

It is somewhat surprising that the molecular flux through the nanopores modified with the shorter polymer brush is smaller than the flux through the nanopores modified with long polymer chains. We speculate that this is the result of the short polymer brush being densely packed and thus forcing diffusion through the free volume of the nanopores, while in the second case diffusion occurs through the entire volume of the nanopores filled with highly permeable amorphous PNIPAAAM.

Similar temperature-response behavior has been reported for PNIPAAAM grafted onto the surface of porous polymer membranes^{11,12,39,40} In those studies different grafting density was proposed to be the reason for the observed variation in the temperature response. To the best of our knowledge, our observations together with the four reports mentioned above are the only examples of the negative temperature response of a PNIPAAAM-based membrane. Negative gating has also been achieved by filling the pores in polymer membranes with poly-(acrylamide)/poly(acrylic acid) hydrogels.⁴¹ In our case, however, switching between the positive and the negative temperature behavior was achieved simply by extending the polymerization time from 15 to 30 min.

Conclusions

We demonstrated that surface-initiated ATRP of *N*-isopropylacrylamide inside colloidal films does not perturb the colloidal

lattice and leads to temperature-responsive colloidal nanopores. Nanopores modified with a thin PNIPAAAM brush exhibited a positive gating behavior, where diffusion rates increased with increasing temperature. Nanopores modified with a thick PNIPAAAM layer showed a negative gating behavior, where diffusion rates decreased with increasing temperature. This temperature response results from two transport mechanisms, one in which molecules diffuse through the nanopore whose volume increases with increasing temperature as PNIPAAAM brush collapses onto the nanopore surface (positive gating) and the other where molecules diffuse through a porous PNIPAAAM filling the entire nanopore opening and collapsing onto itself to become hydrophobic and impermeable (negative gating). The switch between the positive and negative gating could be easily achieved by extending the polymerization time from 15 to 30 min. We are presently studying temperature-responsive PNIPAAAM-modified suspended⁴² and free-standing colloidal membranes as well as nanoporous colloidal films modified with other responsive polymers.

Acknowledgment. This work was supported in part by the NSF CAREER Award, NSF CHE-0616505, and the United States–Israel Binational Science Foundation (BSF). I.Z. is grateful to the Camille and Henry Dreyfus Foundation for a New Faculty Award. We would like to thank Prof. Jakub Nalaskowski (Metallurgical Engineering Department, University of Utah) for help with DLS measurements. MALDI-TOF MS spectra have been obtained at the mass spectrometry facilities of the Chemistry Department, University of Arizona (grant no. NIH S10RR13818).

LA702008J

(39) Park, Y. S.; Ito, Y.; Imanishi, Y. *Langmuir* **1998**, *14*, 910–914.

(40) Chu, L.-Y.; Niitsuma, T.; Yamaguchi, T.; Nakao, S. *AIChE J.* **2003**, *49*, 896–909.

(41) Chu, L.-Y.; Li, Y.; Zhu, J.-H.; Chen, W.-M. *Angew. Chem., Int. Ed.* **2005**, *44*, 2124–2127.

(42) Bohaty, A. K.; Zharov, I. *Langmuir* **2006**, *22*, 5533–5536.